Published in final edited form as:
Alcohol Clin Exp Res. 2014 May ; 38(5): 1255–1265. doi:10.1111/acer.12360.

An Evolutionarily-Conserved Mechanism of Calcium-Dependent Neurotoxicity in a Zebrafish Model of FASD

George R. Flentke[1], **Rebekah H. Klingler**[2], **Robert L. Tanguay**[3], **Michael J. Carvan 3rd**[2], and **Susan M. Smith**[1]

[1]Dept. Nutritional Sciences, Univ. Wisconsin-Madison, Madison WI

[2]School of Freshwater Sciences, Univ. Wisconsin-Milwaukee, Milwaukee WI

[3]Dept. Molecular Environmental Toxicology, Oregon State Univ., Corvallis OR

Abstract

Background—Fetal Alcohol Spectrum Disorders (FASD) are a leading cause of neurodevelopmental disability. Non-human animal models offer novel insights into its underlying mechanisms. Although the developing zebrafish has great promise for FASD research, a significant challenge to its wider adoption is the paucity of clear, mechanistic parallels between its ethanol responses and those of non-piscine, established models. Inconsistencies in the published pharmodynamics for ethanol-exposed zebrafish, alongside the use of comparatively high ethanol doses, challenge the interpretation of this model's clinical relevance.

Methods—To address these limitations, we developed a binge, single-exposure model of ethanol exposure in the early zebrafish embryo.

Results—Brief (3hr) ethanol exposure is sufficient to cause significant neural crest losses and craniofacial alterations, with peak vulnerability during neurogenesis and early somitogenesis. These losses are apoptotic, documented using TUNEL assay and *secA5-YFP*-reporter fish. Apoptosis is dose-dependent with an EC50 = 56.2mM ± 14.3mM ethanol$_{int}$, a clinically-relevant value within the range producing apoptosis in chick and mouse neural crest. This apoptosis requires the calcium-dependent activation of CaMKII and recapitulates the well-described ethanol signaling mechanism in avian neural crest. Importantly, we resolve the existing confusion regarding zebrafish ethanol kinetics. We show that steady-state ethanol concentrations within both chorion-intact and dechorionated embryos are maintained at 35.7% ± 2.8% of ethanol$_{ext}$ levels across the range from 50 to 300 mM ethanol$_{ext}$, a value consistent with several published reports. Equilibrium is rapid and complete within 5min of ethanol addition.

Conclusions—The calcium/CaMKII mechanism of ethanol's neurotoxicity is shared between an amniote (chick) and teleost fish, indicating this mechanism is evolutionarily conserved. Our data suggest that ethanol$_{ext}$ concentrations greater than 2% (v/v) for chorion-intact and 1.5% (v/v) for dechorionated embryos have limited clinical relevance. The strong parallels with established models endorse the zebrafish's relevance for mechanistic studies of ethanol's developmental neurotoxicity.

Communicating Author: Susan Smith, Ph.D., Department of Nutritional Sciences, University of Wisconsin-Madison, 1415 Linden Drive, Madison, WI 53706, Tel (608) 263-4316, Fax (608) 262-5860, suesmith@nutrisci.wisc.edu.

Keywords

Fetal alcohol spectrum disorders; zebrafish; neural crest; apoptosis; calcium signaling; ethanol

Introduction

Fetal Alcohol Spectrum Disorders (FASD) are a leading cause of neurodevelopmental disability, affecting 5–50 /1000 live births (Clarren et al., 2001, May et al., 2009). Although a major consequence of prenatal alcohol exposure is a consistent constellation of behavioral and cognitive deficits, individuals can also display growth deficits and neurocristopathies (Medicine, 1996). Mechanistic studies of ethanol's action within the embryo and fetus have informed these pathologies. One susceptible cell population is the neural crest, a pluripotent stem cell population that contributes to neuronal, connective tissue, and other cranial elements. Ethanol's disruption of neural crest development produces a distinctive facial appearance having diagnostic utility for FASD (Moore et al., 2007). These characteristic neurocristopathies result, in part, from ethanol's well-documented apoptosis of neural crest progenitors (Dunty et al., 2001, Cartwright et al., 1998). Work from our laboratory has detailed the mechanism underlying this apoptosis and it is now a well-understood model of ethanol's neurotoxicity. Within premigratory neural crest progenitors, pharmacologically relevant ethanol concentrations (EC50=52mM) initiate a significant rise in intracellular calcium that originates from G-protein-coupled signaling via phospholipase C and inositol phosphate (Debelak-Kragtorp et al., 2003, Garic-Stankovic et al., 2005). This calcium transient activates the intracellular protein kinase CaMKII, converting the calcium transient into a lasting effector of neural crest fate (Garic et al., 2011). CaMKII also destabilizes the transcriptional effector nuclear β-catenin to ablate canonical Wnt signaling and initiate apoptosis (Flentke et al., 2011, 2013).

Non-human animal models offer insights into the mechanisms and pathologies underlying FASD. A relatively new model for FASD research is the developing zebrafish (*Danio rerio*). Zebrafish embryos are transparent, develop rapidly, and are amenable to genetic manipulation. They have proven power for studying mechanisms of normal and abnormal development including FASD because these morphogenetic mechanisms are largely conserved with other vertebrates including humans (Lieschke and Currie, 2007). Developmental ethanol exposure in zebrafish produces behavioral deficits and dysmorphologies that parallel those of FASD (Tanguay and Reimers, 2008, Carvan et al., 2004, Bilotta et al., 2004, Fernandes and Gerlai, 2009). However, a significant challenges to its wider adoption in FASD research is the paucity of studies that draw clear, mechanistic parallels between the ethanol responses of zebrafish and those of established FASD models. Additionally, published experimental approaches have a propensity to use ethanol concentrations are appreciably greater than those used in other animal models or experienced in human exposure, making it difficult to interpret the study's clinical relevance.

To address these limitations, here we present a binge, single exposure zebrafish model of embryonic ethanol exposure. We demonstrate that ethanol-induced cell death within this model is evolutionarily conserved and parallels the mechanism previously documented in

chick. We also characterize the ethanol delivery kinetics within this model and resolve the existing confusion regarding zebrafish ethanol exposures.

Methods

Zebrafish Husbandry and Embryo Production

Wildtype zebrafish (*Danio rerio*) of strain 5D (Sinnhuber Aquatic Research Laboratory, Oregon State University) or AB (School of Freshwater Sciences, University of Wisconsin-Milwaukee) were raised under standard conditions (28ºC, 14h light/10h dark cycle) as described (Westerfield, 2007). Fertilized eggs (less than 2 hours post-fertilization, hpf) were maintained in Embryo Media (EM), omitting methylene blue, until attaining the desired developmental stage. All experiments used embryos from a single group spawn and treatment assignments were randomized. Unless specifically indicated, all embryos were dechorionated using pronase treatment (127 μg/ml, 30 min; (Mandrell et al., 2012) prior to study. All experimental procedures were approved by the Animal Care and Use Committees of the respective institutions.

Ethanol Treatment

Ethanol concentrations herein are reported as molar and %(v/v). Studies modeled a single binge ethanol exposure at specified times between gastrulation thru early organogenesis. Embryos were staged according to established criteria (Kimmel et al., 1995) and were incubated in 6-well culture plates containing ≤23 embryos/well (5 embryos/ml). Embryos were exposed to either EM or ethanol (200 proof, USP grade, AAPER, Shelbyville, KY) diluted in EM for 3h with gentle rocking. All solutions were then replaced with fresh EM-only and embryos were incubated until the desired experimental endpoint.

Ethanol Quantification

Chorion-intact (25 per sample) or dechorionated (100 per sample) embryos at 8–11hpf were incubated with 0, 50, 100, 200, or 300 mM ethanol, diluted in EM, for experimentally determined times. Embryos were then transferred to a 1.5ml microfuge tube. The excess liquid was carefully decanted, 50 μl EM was added to the tube and immediately removed as a brief wash. Embryos were then flash frozen and stored at -80ºC until analysis. The entire preparation process took ≤30 sec per sample. To quantify ethanol, embryos were homogenized in 4% perchloric acid buffered in 0.5M K_2CO_3, centrifuged, and analyzed in triplicate using the Analox GM-7 Micro-Stat (Lunenburg, MA) using the manufacturer's directions for blood and urine.

To determine embryo volume, we photographed 6hpf embryos at equivalent magnification. Because 6hpf embryos plus intact chorion are essentially spherical, we used their diameter to calculate mean volume. The 6hpf embryo + yolk, *sans* chorion, is somewhat oblong. Therefore, we measured diameters across the major rostrocaudal and dorsoventral axes and used their average to calculate the approximate volume of embryo + yolk. Values are the mean ± SD of 100 embryos.

Cell Death Assessment

Cell death was evaluated using three distinct techniques. For overall cell death, embryos were incubated in 5μg/ml acridine orange (Sigma, St. Louis MO), washed, and imaged. An alternate apoptosis indicator, Lysotracker Red, was problematic because the dye rapidly transferred to the lipid-rich yolk upon fixation. Cleaved DNA end fragments within apoptotic cells were detected using the terminal deoxynucleotidyl transferase-mediated dUTP Nick-End Labeling (TUNEL) fluorescent assay kit (DeadEnd™, Promega, Madison, WI). Apoptosis was independently quantified using the Annexin V reporter zebrafish line Tg(UAS:SEC-Hsa.ANXA5-YFP,myl7:RFP)^{F12}, which expresses secreted YFP-Annexin V in apoptotic cells (van Ham et al., 2010). Embryos were treated with ethanol (media concentration 265mM, internal concentration 95mM) and YFP expression was imaged 4hr later; this shorter time was determined experimentally because extracellular Annexin V precedes the appearance of cleaved DNA fragments. For the inhibitor studies, dechorionated embryos were preincubated 30min with the inhibitor or DMSO carrier (≤0.1%), washed, and treated with ethanol as above. Inhibitors were the intracellular calcium chelator BAPTA-AM (20 μM), calmodulin antagonist calmidizolium (20 nM), and CaMKII inhibitor myristolated-AIP (1 μM, all from Sigma); concentrations were determined experimentally. Experiments used 12–24 embryos per treatment group and were performed in independent replicates or triplicates.

Neural Crest Analysis

Neural crest populations were visualized using *in situ* hybridization of fixed embryos using antisense riboprobe directed against zebrafish neural crest marker *crestin* (gift of Paul Henion, (Luo et al., 2001). *In situ* hybridization used an established method (Thisse and Thisse, 2008) with minor modifications. The signal was visualized under fluorescence using Fast Red TR/Napthol AS-MX (Sigma, St. Louis, MO).

Skeletal Analysis

Embryos at 75% epiboly were exposed to 86mM ethanol as above, and cranial skeletal structures were evaluated at 6-days post-fertilization, just prior to when fry transition to oral feeding. Larvae were stained for cartilage (Carvan et al. 2004), embedded in 3% methylcellulose, and photographed under uniform magnification in ventral, dorsal, and lateral views. Cranial skeletal elements, defined as described (Schilling et al., 1996), were quantified from digital images using ImageJ (Carvan et al. 2004), analyzing 12–14 larvae per treatment group.

Statistical Analysis

Data were tested for normalcy and analyzed using the appropriate statistical test (SigmaStat) with $p<0.05$ being the level of significance. Results are mean ± SD or SEM as indicated.

Results

Embryonic Ethanol Kinetics

In zebrafish, neurodevelopmental events between 6hpf (convergent extension begins) and 11hpf (3 somites) are developmentally comparable to the chick embryo stages (gastrulation through neural fold stages) in which we have extensively documented the ethanol-mediated cell death within early neural and neural crest progenitors (Kimmel et al., 1995, Kimmel et al., 2001). We calculated that the chorionated egg containing a 6hpf AB embryo had a mean volume (± SD) of 882 nl ± 120 nl, a value consistent with Hagedorn et al. (1998). For embryos having an intact chorion, ethanol uptake was linear across the range of external ethanol concentrations ($ethanol_{ext}$) from 0 mM to 300 mM ethanol in the media (Figure 1A). Within this range, the egg's internal ethanol concentration ($ethanol_{int}$) averaged 36% of $ethanol_{ext}$ in which the egg was incubated, a value in agreement with that published elsewhere (30%, (Reimers et al., 2004a). Dechorionated 6hpf embryos plus yolk had a calculated mean volume ± SD of 219 nl ± 30 nl, consistent with published values (Hagedorn et al., 1998, Bradfield et al., 2006). The ethanol partitioning profile for dechorionated embryos was essentially indistinguishable from that of chorion-intact embryos, and mean internal ethanol concentrations averaged 35% of $ethanol_{ext}$ across the range from 50–300 mM (Figure 1B).

For embryos with intact chorions, time course analyses revealed that ethanol equilibrated rapidly between the embryo and medium and reached steady-state concentrations within 15min of ethanol addition (Figure 1C). The ratio of $ethanol_{int}$ to $ethanol_{ext}$ in these embryos remained steady at 35.7% ± 2.8% for at least 8hr of continuous ethanol exposure and the steady-state ratio did not vary as a function of $ethanol_{ext}$ (Figure 1D).

We also evaluated the impact of washing upon ethanol content. For chorionated embryos, a 60-second incubation in ethanol-free medium reduced their ethanol content by 50% (54.2% ± 3.1%, mean ± SEM). After two 60-second washes, $ethanol_{int}$ was only 20.4% of the starting value (Table 1).

Cell Death is Dose- and Stage-Dependent

Acridine orange (AO) is used extensively to monitor cell death in FASD models including zebrafish (Reimers et al., 2006, Loucks and Carvan, 2004, Cartwright and Smith, 1995, Kashyap et al., 2011). We used it to characterize the dose- and stage-dependence of cell death in this short-exposure binge model. In control embryos incubated in media from 75% epiboly onward, we consistently observed small numbers of AO^+ cells within cranial, ocular, tail bud, and somite regions (Figure 2A). Ethanol (86 mM $ethanol_{ext}$) increased the number of AO^+ cells within these same regions and especially within cranial populations including the cranial mesenchyme, neural folds and ocular tissue (arrows, Figure 2B). This cell-labeling pattern paralleled that described for similarly-staged, ethanol-treated chick and mouse embryos (Dunty et al. 2000; Cartwright and Smith 1995). This ethanol level did not appreciably delay the embryo's developmental trajectory.

As with comparably-staged chick and mouse, ethanol's induction of cell death was dose-dependent. $Ethanol_{ext}$ levels from 28 to 344 mM (0.16% to 2.0%, v/v) significantly

increased the number of AO^+ cells within presumptive cranial regions at 10–12 hpf, the stage at which cranial neural crest specification is complete and migration begins (Kimmel et al., 1995, Schilling and Kimmel, 1994). Enumeration revealed increased AO^+ cell numbers at exposures as low as 28 mM $ethanol_{ext}$ and significantly exceeded control values at 55 mM (0.33%) $ethanol_{ext}$ and greater (Figure 2C). The data best modeled ($F=162.4$, $p<0.0001$) a hyperbola with a non-zero baseline (21.2 ± 4.5 AO^+ cells). From these data we calculated an EC50 for cell death of 56.2 mM ± 14.3 mM $ethanol_{int}$ (156.1 mM ± 39.8 mM $ethanol_{ext}$), a value similar to the calculated EC50 (52 mM) for comparably-staged chick embryos (Garic-Stankovic et al., 2005). Peak numbers of labeled cells occurred between 5hr to 6hr following ethanol addition (data not shown). Within this 5hr time period, ethanol treatment did not adversely affect short-term embryo survival until $ethanol_{ext}$ was 516 mM (3%), wherein 100% mortality was observed. Overall, the concentration range of zebrafish sensitivity to cell death strongly paralleled that described for our chick embryo model (Cartwright and Smith, 1995, Debelak and Smith, 2000). Based on these findings, we selected 86mM $ethanol_{ext}$ (0.5% v/v $ethanol_{ext}$; 31mM $ethanol_{int}$) for subsequent investigation.

Sensitivity of cranial populations to cell death depended upon the embryo's developmental stage. We surveyed the period from gastrulation (50%-epiboly, 5.3hpf) through neural keel formation (8-somite, 13hpf), a period that parallels chick gastrulation through neural-fold fusion and the onset of neural crest migration. The greatest cranial cell death occurred when ethanol exposure was initiated at 75%- to 90%-epiboly (8–9 hpf), and levels were somewhat lower before and after this exposure time (Figure 2D). Cell death significantly exceeded that of controls at all four developmental periods ($p<0.05$), and control levels declined as the embryo matured. Therefore we selected ethanol exposure from 75%-epiboly (8hpf) to the 3-somite stage (11hpf) for subsequent investigation, as these stages displayed the strongest ethanol-induced cell death relative to background levels within cranial progenitors.

Ethanol-Induced Cell Death is Apoptotic

We used two distinct methods, TUNEL labeling and Annexin V-labeling of phosphatidylserine, to confirm that the signal detected by acridine orange represented apoptosis (Krysko et al., 2008). Annexin-V is a calcium-dependent protein that binds phosphatidylserine (PS) with high affinity and reflects the inability to maintain membrane asymmetry during the early steps of apoptosis (Vermes et al., 1995). We used the *secA5-YFP* transgenic zebrafish line, in which secreted Annexin V is fused to yellow fluorescent protein, to detect extracellular PS and thus apoptosis in real-time (van Ham et al., 2010). Ethanol treatment caused a three-fold elevation in the number of secA5-YFP^+ cells within the early cranial region, and this difference was significant ($p<0.001$; Figure 3A, 3B, 3F). High magnification of secA5-YFP^+ cells revealed both the characteristic pyknotic fragmentation that is characteristic of apoptosis, and the “ring” structure of the Annexin V-PS interaction at the cell membrane (inset, Figure 3B). The TUNEL technique uses terminal deoxynucleotidyl transferase to add a tagged nucleotide to the cleaved nuclear DNA ends that are a late characteristic of the apoptosis cascade. Consistent with the Annexin V findings, the number of $TUNEL^+$ cells also increased nearly three-fold within ethanol-treated cranial regions ($p<0.001$, Figures 3C, 3D, 3G). Many labeled cells had the

characteristic pyknotic appearance of apoptosis. We conclude that the cell death detected by acridine orange in ethanol-treated zebrafish embryos is largely apoptotic.

Ethanol-Induced Apoptosis is Calcium/CaMKII-Dependent

The apoptosis of chick neural crest progenitors uses a well-documented mechanism involving the ethanol-mediated mobilization of intracellular calcium and subsequent activation of CaMKII (Debelak-Kragtorp et al., 2003, Garic-Stankovic et al., 2005, Garic et al., 2011). To test if this pathway also contributes to apoptosis in zebrafish, we investigated three calcium-dependent steps in this chick apoptosis pathway: calcium release, and the downstream involvement of calmodulin and CaMKII. Pretreatment of zebrafish embryos with the intracellular calcium chelator Bapta-AM prevented the ethanol-induced apoptosis and restored it to levels indistinguishable from those of controls ($p<0.006$ vs. ethanol-only; Figure 4A–C, Figure 5). The cytosolic protein calmodulin is an intracellular calcium sensor that activates numerous calcium-dependent protein kinases including CaMKII. The small molecule calmidizolium, a reversible calmodulin antagonist, prevented the ethanol-induced apoptosis in zebrafish cranial progenitors ($p<0.001$ vs. ethanol-only; Figure 4D, Figure 5), as did the peptide myristoylated-AIP (myrAIP), which inhibits CaMKII autophosphorylation and thus its activation ($p<0.001$ vs. ethanol-only; Figure 4E, Figure 5). MyrAIP also blocked apoptosis as revealed by TUNEL staining (Figure 4E) and further confirmed the apoptotic mechanism. The calcium chelator Bapta-AM, but not calmodulin or myrAIP, significantly reduced cell death in controls ($p=0.041$ vs control-only, Figure 5), suggesting this endogenous cell death was calcium-dependent but did not involve CaMKII.

Ethanol Reduces Neural Crest Numbers

To ascertain whether this apoptosis affected neural crest survival, we quantified these populations through their expression of *crestin*, a protein of unknown function that is induced early during neural crest development (Luo et al., 2001). Ethanol treatment significantly reduced the number of *crestin*$^{+}$ cells within cranial regions ($p<0.001$; Figure 6A, 6B) to levels that were only 58% of control values (Figure 6C). Losses were greatest within populations emerging from the midbrain and anterior hindbrain (arrows, Figure 6B). Neural crest populations caudal to the otic vesicle appeared to be less severely affected, and this might reflect the timing of ethanol treatment because those populations are slightly younger than more cranial populations.

At 6-days post-fertilization, this brief ethanol exposure model altered several elements of the neural crest-derived cranial skeleton. In the lower jaw, the mandibular cartilage dimensions were narrowed (Figure 7; $p = 0.041$, control 379 μm ± 23 μm, ethanol 362 μm ± 23 μm, 95.5% ± 6.2% of control) and elongated ($p = 0.00011$, control 206 μm ± 20 μm, ethanol 244 μm ± 22 μm, 118% ± 11% of control) by ethanol treatment. Within the upper jaw, the ethmoid plate was shortened by ethanol treatment ($p = 0.0029$, control 314 μm ± 14 μm, ethanol 288 μm ± 24 μm, 91.9% ± 7.6% of control), and width across the trabeculae cranii was increased ($p = 0.011$, control 299 μm ± 18 μm, ethanol 321 μm ± 21 μm, 107.5% ± 7.2% of control). Other cranial skeletal elements, as well as body length, did not significantly differ.

Discussion

The zebrafish is a powerful developmental model due to its rapid development, transparency, and ease of genetic manipulation. Unfortunately its potential for FASD research is not fully realized due to the lack of clear mechanistic parallels between its ethanol responses and those of established research models. Additionally, the zebrafish FASD literature is confounded by an extreme range of ethanol exposure values, and thus the pharmacologically-relevant ethanol dosage remains unclear. We address several of these limitations in presenting a binge, single-exposure model of embryonic ethanol exposure that recapitulates multiple aspects of established avian and murine models. We show that clinically relevant ethanol concentrations cause the apoptosis of early neural progenitors including neural crest within zebrafish, as well as craniofacial alterations, at ethanol levels similar to those for mouse and chick. We verify that the mechanism of early neural apoptosis requires intracellular calcium and CaMKII activity, a mechanism also used in chick and demonstrating that this mechanism of ethanol action is evolutionarily conserved. Finally, we resolve the substantial confusion in the zebrafish literature regarding ethanol exposures. We quantify the embryos' ethanol content and confirm independent findings that show a steady-state ethanol content within the embryo ($ethanol_{int}$) at 35.7% ± 2.8% of external ethanol concentrations ($ethanol_{ext}$). Moreover, ethanol equilibrates rapidly, both in the presence and absence of the chorion. Validation of zebrafish against other FASD models enhances this model's utility to address mechanistic, genetic, and other research questions emerging from other established models.

Ethanol Dosage in Zebrafish

Perhaps the single greatest barrier to the wider adoption of zebrafish as an ethanol research model is the question of ethanol pharmacodynamics and the actual ethanol levels experienced by the embryo. Published embryo studies have utilized $ethanol_{ext}$ as high as 400 mM to 1.6M (10%v/v) and $ethanol_{ext}$ of 344 mM (2%v/v) to 500 mM (3%v/v) are common (Ali et al., 2011, Bilotta et al., 2004, Blader and Strahle, 1998, Li et al., 2007, Loucks and Ahlgren, 2009, Sylvain et al., 2010, Zhang et al., 2010). These high $ethanol_{ext}$ levels were justified by reports of steep external-to-internal gradients ranging from 25-fold to nearly 3,000-fold (Ali et al., 2011, Fernandes and Gerlai, 2009, Li et al., 2007). The wide variation in those calculated ratios suggests significant methodological inconsistencies in their determination. We found that half the internal ethanol content is removed during a 60-second wash, a phenomenon noted elsewhere (Zhang et al. 2013). We suggest that the inconsistencies in past attempts to quantify ethanol content likely resulted from their use of multiple washes. We also found that the chorion is less of a barrier to ethanol than previously assumed. Using a single, rapid wash and total wash-to-freeze time of <30sec, we found that the $ethanol_{int}$ for embryos having intact chorions averaged 35.7% ± 2.8% of external levels, a partitioning value that is within the range of work using similarly aged embryos and either alternative enzymatic-based methodologies (30%, Reimers et al., 2004a; 30%–32%, Zhang et al., 2013) or gas chromatography (48% – 56%; Lovely, et al. submitted). For dechorionated embryos, the partitioning between media and tissue was again 35% and within the range reported by Cole (19%, Zhang et al., 2013), Tanguay (30%, pers. comm.) and Lovely et al. (24% – 37%, submitted). Thus, as suggested by Blader using a

phenotypic endpoint, the chorion is not a substantial kinetic barrier to ethanol transport (Blader and Strahle, 1998). Ethanol equilibration across the chorion, and between the embryo and its external environment, was rapid and achieved steady-state well under 15 minutes over a wide range of ethanol concentrations. Unlike Bradfield et al. (2006) we saw no ethanol build-up over time, and ethanol equilibration was maintained at 35% to 36% over an 8-hour exposure period.

From these data, we estimate that for dechorionated embryos ≤24hpf, 1%v/v $ethanol_{ext}$ produces 61.6 mM $ethanol_{int}$, or 284 mg%. For chorion-intact embryos, the situation is more complex because the pharmacokinetic partitioning of ethanol between the intact chorion compartment and embryo is unknown. Assuming that this value is the same as for dechorionated embryos, then 2%v/v (344 mM) $ethanol_{ext}$ would produce an ethanol concentration in the chorion fluid of 0.72%v/v (568 mg%, 124 mM) and within the embryo 0.25%v/v (200 mg%, 43.4 mM). If instead the two compartments are in free equilibria, 2%v/v (344 mM) $ethanol_{ext}$ would produce $ethanol_{int}$ values within both chorion and embryo compartments of 0.72% v/v, or 568 mg% (124 mM). This value is much higher than previously assumed and well above the BACs typically employed in rodent or avian models (100–450 mg%) and observed clinically. Given these findings and those of Lovely et al. (submitted), we recommend that future zebrafish studies refrain from greater than 2%v/v $ethanol_{ext}$ for chorion-intact embryos and 1.5%v/v for dechorionated embryos. In practice, 1%v/v $ethanol_{ext}$ for chorionated embryos and 0.5%v/v for dechorionated embryos would compare favorably with established rodent FASD exposures (142–284 mg%). Additionally, because ethanol equilibration is achieved within 15min, lengthy exposures are unnecessary and, as in rodent and avian studies, the ethanol treatment can be focused upon narrow developmental events lasting minutes to a few hours duration. These values will likely shift depending on the embryo's size, age, and maturational state of ethanol processing machinery; thus, as with mammalian studies, it is important to quantify the actual exposure at the onset of new investigations.

It is unclear how the embryo maintains the linear dose curves up to 8hr over the broad range of ethanol concentrations tested. Zebrafish expresses several alcohol dehydrogenase enzymes as early as 4hpf (Dasmahapatra et al., 2001, Reimers et al., 2004b). Enzymatic metabolism is unlikely to be a sole mechanism to maintain the steady-state gradient. For example, a major alcohol dehydrogenase in the zebrafish embryo, Adh8a, has a Km of 0.7mM for ethanol (Reimers et al., 2004b). Across the ethanol range from 50–300mM, the enzyme would be catalyzing ethanol substrate at 98–99% Vmax, calculated for 1mM NAD. Because cytosolic NAD levels average 0.3mM (Yamada et al., 2006) maintaining a 35% gradient would deplete NAD to levels incompatible with embryo growth and survival, and we did not observe appreciable growth retardation or embryo mortality. While ABC active transporters and other ethanol metabolizing enzymes (Cyp2e1) exist in zebrafish (Dean and Annilo, 2005, Passeri et al., 2009), these or other active transport systems have the same energetic and enzymatic limitations as the alcohol dehydrogenases. Passive transport, such as that effected through aquaglyceroporin family members that reduce intracellular ethanol in yeast, offer a less energy-limiting strategy to maintain steady-state ethanol over a prolonged period (Teixeira et al., 2009). Aquaglyceroporins have been identified in

zebrafish but their ethanol transport capacity and embryonic expression are uncharacterized (Hamdi et al., 2009).

Neural Crest Apoptosis is Conserved in Chick and Zebrafish

While apoptosis is a well-characterized mechanism of ethanol-induced damage in mammalian and avian FASD models (Dunty et al., 2001, Cartwright et al., 1998), the similarity of these mechanisms in zebrafish is unclear. Ethanol exposures from 10mM to 300mM cause extensive cell death when treated from 0hpf to 24hpf, as detected using acridine orange (Carvan et al., 2004, Loucks and Carvan, 2004) and TUNEL (Reimers et al., 2006). We find similar cell death enrichment in cranial and ocular regions, and extend their work to show that even brief ethanol exposure produces appreciable cell death and neural crest losses. We further document this acridine orange signal represents apoptosis using both early markers (annexin-V reporter) and late endpoints (TUNEL) of the apoptotic progression. This mechanism is consistent with our work in the avian model (Cartwright et al., 1998) and the distribution and magnitude of neural crest losses are comparable. Thus this brief, binge exposure model is appropriate for mechanistic studies of apoptotic death in neural crest.

Unlike the more commonly used long-exposure models, this brief exposure model enabled us to define developmental windows for neural crest that are vulnerable to ethanol-mediated apoptosis. Focused ethanol exposure from 75% epiboly (8hpf) to 3-somites (11hpf) caused the most craniofacial apoptosis relative to controls. This period encompasses premigratory events involving the induction, specification, and determination of neural crest progenitors along the neuroectoderm border (Schilling and Kimmel, 1994, Kimmel et al., 1995, Kimmel et al., 2001). During the 2hrs following ethanol removal, the neural keel forms and cranial neural crest initiates migration into the facial anlage. These events directly parallel the vulnerable events previously described for chick neural crest, which span the period from gastrulation (stage 4) to the onset of migration (10 somites) (Cartwright and Smith, 1995) and further endorses that the underlying mechanisms are conserved. Consistent with studies using longer ethanol exposures, this brief ethanol exposure also produced craniofacial defects that parallel other FASD models (Carvan et al., 2004, Bilotta et al., 2004, Zhang et al., 2011, Dlugos and Rabin, 2007).

Finally, we show that key elements of neural crest apoptosis, originally defined in chick, are also present in zebrafish neural crest. The calculated EC50 for ethanol-induced apoptosis in these zebrafish embryos was 56.2mM ± 14.3mM $ethanol_{int}$, a value that is comparable to the 52mM ethanol dose eliciting half-maximal calcium release in chick neural crest (Garic-Stankovic et al., 2006). As with the avian model, the ethanol-mediated apoptosis of zebrafish neural crest requires intracellular calcium and calmodulin-dependent CaMKII activity (Debelak-Kragtorp et al., 2003; Flentke et al., 2011; Garic et al., 2011, Garic-Stankovic et al., 2005). Thus several major components of this well-described cell death pathway are intact in zebrafish, suggesting this mechanism of ethanol's neurotoxicity is evolutionarily conserved between an amniote (*Gallus gallus*) and a vertebrate non-amniote (*Danio rerio*) species. This is one of the first direct comparisons of ethanol responsiveness between zebrafish and established non-piscine FASD models at the mechanistic level. Taken

together, the comparable dose-response range, window of sensitivity, and mechanism of neural crest apoptosis affirm that ethanol vulnerabilities are similar between chick and zebrafish, and at ethanol concentrations similar to those of mammalian and avian FASD models. While avian embryos are important models for neural crest and FASD research, their narrow genetic accessibility relative to mouse and zebrafish limits their investigative utility. These findings validate the short-exposure zebrafish model for deeper mechanistic studies of this ethanol-mediated apoptosis pathway, and especially the study of genetic factors that modify vulnerability to ethanol-induced damage.

Acknowledgments

Supported by NIH R37 AA11085 (S.M.S.), NIH P30 ES000210 (R.L.T.), and a Chancellors' Award from UW-Madison and UW-Milwaukee (S.M.S. and M.J.C., 3rd). We thank Carrie Barton, Cari Buchner and Jane LaDu for outstanding advice and technical support, and Martin Widdowson for advice about zebrafish ethanol quantitation using Analox methodology. We are especially grateful to Ben Lovely and Johann Eberhardt for generously sharing their prepublication data on ethanol pharmokinetics.

References

Ali S, Champagne DL, Alia A, Richardson MK. Large-scale analysis of acute ethanol exposure in zebrafish development: a critical time window and resilience. PLoS One. 2011; 6:e20037. [PubMed: 21625530]

Battaglia, FC. Fetal alcohol syndrome diagnosis, epidimiology, prevention and treatment. Washington, D.C: National Academy Press; 1996.

Bilotta J, Barnett JA, Hancock L, Saszik S. Ethanol exposure alters zebrafish development: a novel model of fetal alcohol syndrome. Neurotox Teratol. 2004; 26:737–743.

Blader P, Strahle U. Ethanol impairs migration of the prechordal plate in the zebrafish embryo. Dev Biol. 1998; 201:185–201. [PubMed: 9740658]

Bradfield JY, West JR, Maider SE. Uptake and elimination of ethanol by young zebrafish embryos. Neurotox Teratol. 2006; 28:629–633.

Cartwright MM, Smith SM. Stage-dependent effects of ethanol on cranial neural crest cell development: partial basis for the phenotypic variations observed in fetal alcohol syndrome. Alcohol Clin Exp Res. 1995; 19:1454–1462. [PubMed: 8749810]

Cartwright MM, Tessmer LL, Smith SM. Ethanol-induced neural crest apoptosis is coincident with their endogenous death, but is mechanistically distinct. Alcohol Clin Exp Res. 1998; 22:142–149. [PubMed: 9514299]

Carvan MJ 3rd, Loucks E, Weber DN, Williams FE. Ethanol effects on the developing zebrafish: neurobehavior and skeletal morphogenesis. Neurotox Teratol. 2004; 26:757–768.

Clarren SK, Randels SP, Sanderson MM, Fineman RM. Screening for fetal alcohol syndrome in primary schools: a feasibility study. Teratology. 2001; 63:3–10. [PubMed: 11169548]

Dasmahapatra AK, Doucet HL, Bhattacharya C, Carvan MJ 3rd. Developmental expression of alcohol dehydrogenase (ADH3) in zebrafish (Danio rerio). Biochem Biophys Res Commun. 2001; 286:1082–1086. [PubMed: 11527411]

Dan M, Annilo T. Evolution of the ATP-binding cassette (ABC) transporter superfamily in vertebrates. Annu Rev Genomics Hum Genet. 2005; 6:123–142. [PubMed: 16124856]

Debelak-Kragtorp KA, Armant DR, Smith SM. Ethanol-induced cephalic apoptosis requires phospholipase C-dependent intracellular calcium signaling. Alcohol Clin Exp Res. 2003; 27:515–523. [PubMed: 12658119]

Debelak KA, Smith SM. Avian genetic background modulates the neural crest apoptosis induced by ethanol exposure. Alcohol Clin Exp Res. 2000; 24:307–314. [PubMed: 10776667]

Dluglos CA, Rabin RA. Ocular deficits associated with alcohol exposure during zebrafish development. J Comp Neurol. 2007:497–506. [PubMed: 17394139]

Dunty WC Jr, Chen SY, Zucker RM, Dehart DB, Sulik KK. Selective vulnerability of embryonic cell populations to ethanol-induced apoptosis: implications for alcohol-related birth defects and neurodevelopmental disorder. Alcohol Clin Exp Res. 2001; 25:1523–1535. [PubMed: 11696674]

Fernendes Y, Gerlai R. Long-term behavioral changes in response to early developmental exposure to ethanol in zebrafish. Alcohol Clin Exp Res. 2009; 33:601–609. [PubMed: 19183139]

Flentke GR, Garic A, Amberger E, Hernandez M, Smith SM. Calcium-mediated repression of beta-catenin and its transcriptional signaling mediates neural crest cell death in an avian model of fetal alcohol syndrome. Birth Def Res A. 2011; 91:591–602.

Flentke GR, Garic A, Hernandez M, Smith SM. CaMKII Represses Transcriptionally-Active β-Catenin to Mediate Acute Ethanol Neurodegeneration and Can Phosphorylate β-Catenin. J Neurochem. 2013 (in press).

Garic-Stankovic A, Hernandez M, Flentke GR, Smith SM. Structural constraints for alcohol-stimulated Ca2+ release in neural crest, and dual agonist/antagonist properties of n-octanol. Alcohol Clin Exp Res. 2006; 30:552–559. [PubMed: 16499497]

Garic-Stankovic A, Hernandez MR, Chiang PJ, Debelak-Kragtorp KA, Flentke GR, Armant DR, Smith SM. Ethanol triggers neural crest apoptosis through the selective activation of a pertussis toxin-sensitive G protein and a phospholipase Cbeta-dependent Ca2+ transient. Alcohol Clin Exp Res. 2005; 29:1237–1246. [PubMed: 16046880]

Garic A, Flentke GR, Amberger E, Hernandez M, Smith SM. CaMKII activation is a novel effector of alcohol's neurotoxicity in neural crest stem/progenitor cells. J Neurochem. 2011; 118:646–657. [PubMed: 21496022]

Hagedorn M, Kleinhans FW, Artemov D, Pilatus U. Characterization of a major permeability barrier in the zebrafish embryo. Biol Reprod. 1998; 59:1240–1250. [PubMed: 9780333]

Hamdi M, Sanchez MA, Beene LC, Liu Q, Landfear SM, Rosen BP, Liu Z. Arsenic transport by zebrafish aquaglyceroporins. BMC Mol Biol. 2009; 10:104. [PubMed: 19939263]

Kashyap B, Frey RA, Stenkamp DL. Ethanol-induced microphthalmia is not mediated by changes in retinoic acid or sonic hedgehog signaling during retinal neurogenesis. Alcohol Clin Exp Res. 2011; 35:1644–1661. [PubMed: 21554333]

Kimmel CB, Ballard WW, Kimmel SR, Ullmann B, Schilling TF. Stages of embryonic development of the zebrafish. Dev Dyn. 1995; 203:253–310. [PubMed: 8589427]

Kimmel CB, Miller CT, Keynes RJ. Neural crest patterning and the evolution of the jaw. J Anat. 2001; 199:105–120. [PubMed: 11523812]

Krysko DV, Vanden Berghe T, D'Herde K, Vandenabeele P. Apoptosis and necrosis: detection, discrimination and phagocytosis. Methods. 2008; 44:205–21. [PubMed: 18314051]

Li YX, Yang HT, Zdanowicz M, Sicklick JK, Qi Y, Camp TJ, Diehl AM. Fetal alcohol exposure impairs Hedgehog cholesterol modification and signaling. Lab Invest. 2007; 87:231–40. [PubMed: 17237799]

Lieschke GJ, Currie PD. Animal models of human disease: zebrafish swim into view. Nat Rev Genet. 2007; 8:353–367. [PubMed: 17440532]

Loucks E, Carvan MJ 3rd. Strain-dependent effects of developmental ethanol exposure in zebrafish. Neurotox Teratol. 2004; 26:745–755.

Loucks EJ, Ahlgren SC. Deciphering the role of Shh signaling in axial defects produced by ethanol exposure. Birth Def Res A. 2009; 85:556–567.

Luo R, ANM, Arduini BL, Henion PD. Specific pan-neural crest expression of zebrafish Crestin throughout embryonic development. Dev Dyn. 2001; 220:169–174. [PubMed: 11169850]

Mandrell D, Truong L, Jephson C, Sarker RM, Moore A, Lang C, Simonich MT, Tanguay RL. Automated Zebrafish Chorion Removal and Single Embryo Placement: Optimizing Throughput of Zebrafish Developmental Toxicity Screens. J Lab Automat. 2012; 17:66–74.

May PA, Gossage JP, Kalberg WO, Robinson LK, Buckley D, Manning M, Hoyme HE. Prevalence and epidemiologic characteristics of FASD from various research methods with an emphasis on recent in-school studies. Dev Disabil Res Rev. 2009; 15:176–192. [PubMed: 19731384]

Moore ES, Ward RE, Wetherill LF, Rogers JL, Autti-Ramo I, Fagerlund A, Jacobson SW, Robinson LK, Hoyme HE, Mattson SN, Foroud T. CIFASD. Unique facial features distinguish fetal alcohol

syndrome patients and controls in diverse ethnic populations. Alcohol Clin Exp Res. 2007; 31:1707–1713. [PubMed: 17850644]

Passeri MJ, Cinaroglu A, Gao C, Sadler KC. Hepatic steatosis in response to acute alcohol exposure in zebrafish requires sterol regulatory element binding protein activation. Hepatology. 2009; 49:443–452. [PubMed: 19127516]

Reimers MJ, Flockton AR, Tanguay RL. Ethanol- and acetaldehyde-mediated developmental toxicity in zebrafish. Neurotox Teratol. 2004a; 26:769–781.

Reimers MJ, Hahn ME, Tanguay RL. Two zebrafish alcohol dehydrogenases share common ancestry with mammalian class I, II, IV, and V alcohol dehydrogenase genes but have distinct functional characteristics. J Biol Chem. 2004b; 279:38303–38312. [PubMed: 15231826]

Reimers MJ, LaDu JK, Periera CB, Giovanni J, Tanguay RL. Ethanol-dependent toxicity in zebrafish is partially attenuated by antioxidants. Neurotox Teratol. 2006; 28:497–508.

Schilling TF, Kimmel CB. Segment and cell type lineage restrictions during pharyngeal arch development in the zebrafish embryo. Development. 1994; 120:483–494. [PubMed: 8162849]

Sylvain NJ, Brewster DL, Ali DW. Zebrafish embryos exposed to alcohol undergo abnormal development of motor neurons and muscle fibers. Neurotox Teratol. 2010; 32:472–480.

Tanguay RL, Reimers MJ. Analysis of ethanol developmental toxicity in zebrafish. Meth Mol Biol. 2008; 447:63–74.

Teixeira MC, Raposo LR, Mira NP, Lourenco AB, Sa-Correia I. Genome-wide identification of Saccharomyces cerevisiae genes required for maximal tolerance to ethanol. Appl Environ Microbiol. 2009; 75:5761–5772. [PubMed: 19633105]

Thisse C, Thisse B. High-resolution in situ hybridization to whole-mount zebrafish embryos. Nat Protoc. 2008; 3:59–69. [PubMed: 18193022]

Van Ham TJ, Mapes J, Kokel D, Peterson RT. Live imaging of apoptotic cells in zebrafish. FASEB J. 2010; 24:433643–42.

Vermes I, Haanen C, Steffens-Nakken H, Reutelingsperger C. A novel assay for apoptosis. Flow cytometric detection of phosphatidylserine expression on early apoptotic cells using fluorescein labelled Annexin V. J Immunol Meth. 1995; 184:39–51.

Westerfield, M. The Zebrafish Book. University of Oregon Press; Eugene OR: 2007.

Yamada K, Hara N, Shibata T, Osago H, Tsuchiya M. The simultaneous measurement of nicotinamide adenine dinucleotide and related compounds by liquid chromatography/electrospray ionization tandem mass spectrometry. Anal Biochem. 2006; 352:282–285. [PubMed: 16574057]

Zhang C, Ojiaku P, Cole GJ. Forebrain and hindbrain development in zebrafish is sensitive to ethanol exposure involving agrin, Fgf, and sonic hedgehog function. Birth Def Res A. 2013; 97:8–27.

Zhang C, Turton QM, Mackinnon S, Sulik KK, Cole GJ. Agrin function associated with ocular development is a target of ethanol exposure in embryonic zebrafish. Birth Def Res A. 2011; 91:129–141.

Zhang Y, Shao M, Wang L, Liu Z, Gao M, Liu C, Zhang H. Ethanol exposure affects cell movement during gastrulation and induces split axes in zebrafish embryos. Int J Dev Neurosci. 2010; 28:283–288. [PubMed: 20394815]

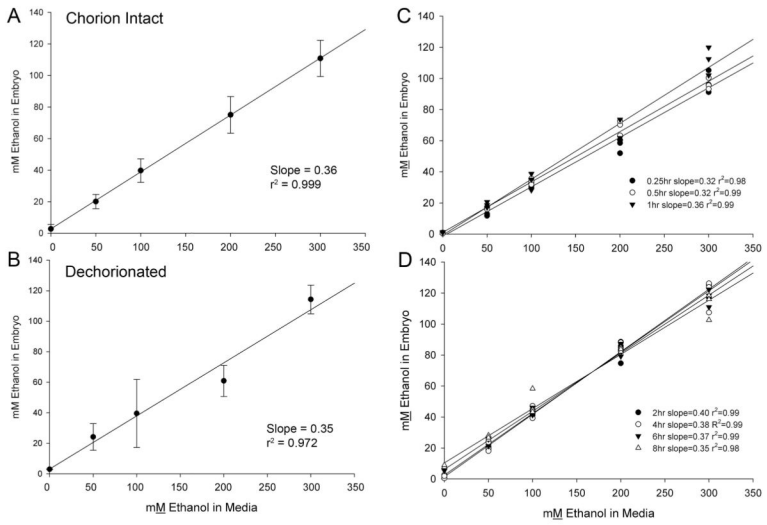

Figure 1. Ethanol Pharmodynamics of Zebrafish Embryos

(A, B) Embryos at 6hpf with chorions intact or removed were incubated 1hr in the indicated ethanol concentration in the media ($ethanol_{ext}$) and the internal ethanol concentration ($ethanol_{int}$) was quantified thereafter. The ratio of $ethanol_{int}/ethanol_{ext}$ concentration was calculated from the slopes by linear regression analysis. For embryos having intact chorions **(A)**, $ethanol_{ext}$ between 50mM to 300 mM yielded $ethanol_{int}$ values that were 36% of $ethanol_{ext}$. For dechorionated embryos **(B)**, $ethanol_{int}$ values were 35% of $ethanol_{ext}$ levels. **(C, D)** Embryos with intact chorions maintain steady-state kinetics of ethanol uptake between 0.25hr and 8hr ethanol exposure. **(C)** $Ethanol_{int}$ levels reached equilibrium with $ethanol_{ext}$ levels within 15min of ethanol exposure and were maintained at those levels for the following hour. **(D)** Between 2hr and 8hr incubation, $ethanol_{int}$ levels were maintained at steady-state values which were 35–36% of $ethanol_{ext}$ values across the entire concentration range of 50–300 mM. Values represent mean ± SD of three independent groups per dose, each having 25 (chorionated) or 100 embryos (dechorionated).

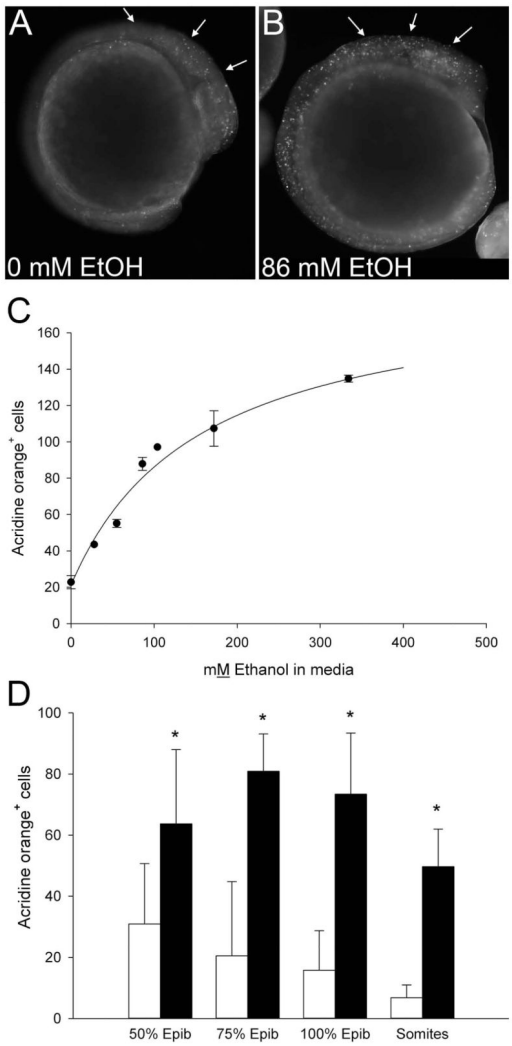

Figure 2. Dose-Dependence and Timing of Ethanol-Induced Cell Death

(A, B) Cell death, visualized using acridine orange, in representative embryos exposed 3hr at neurulation-stage to **(A)** 0mM or **(B)** 86mM ethanol$_{ext}$. Embryos exposed to 86mM ethanol$_{ext}$ at 75% epiboly exhibit numerous labeled cells within developing cranial region (arrows), as well as presomitic and postsomitic mesenchyme. **(C)** Quantitation of dose- dependent cell death in dechorionated embryos (75%–100% epiboly) exposed 3hr to the indicated ethanol$_{ext}$ levels (0, 28, 55, 86, 104, 172, 344mM) and assessed 2hr after ethanol removal. . Data are mean ± SEM. **(D)** Dechorionated embryos were treated with 0mM (open bars) or 86mM ethanol$_{ext}$ (solid bars) at the onset of the indicated stages (somites = 3–6 somites) and cell death was quantified as in **(C)**. Values are mean ± SD with 6–20 embryos per group. * Significantly differs from 0mM ethanol at $p<0.05$, using Kruskal-Wallis one-way ANOVA on ranks and Dunn's pairwise comparison.

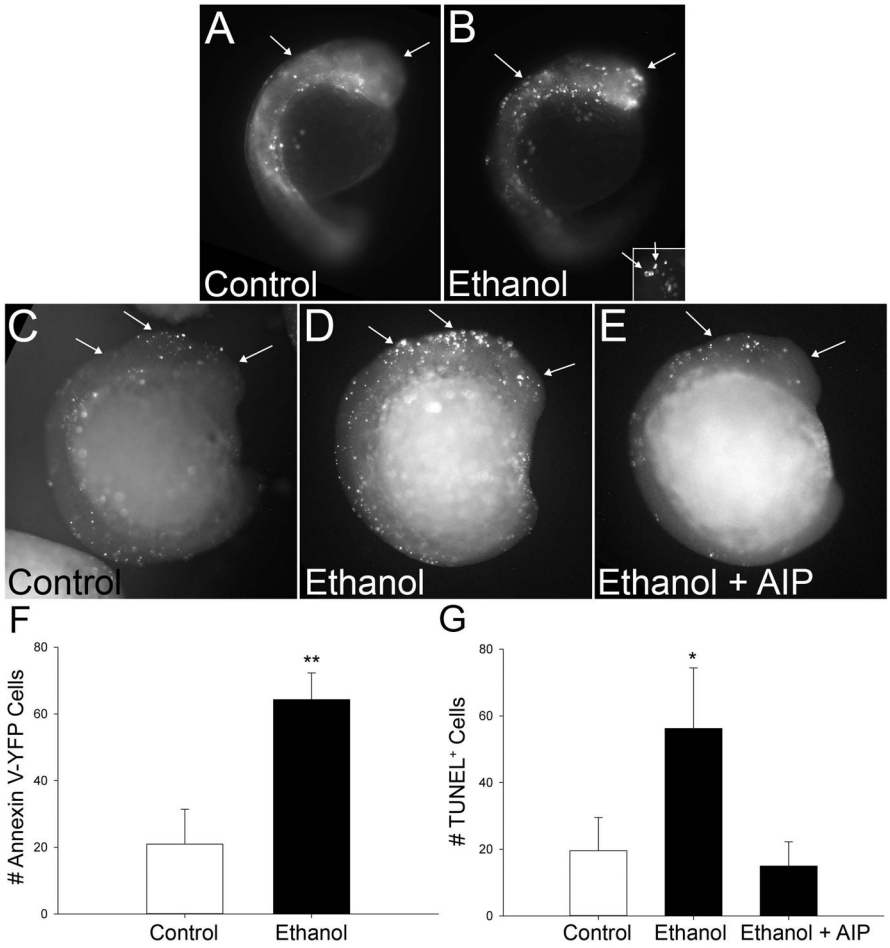

Figure 3. Ethanol-Induced Cell Death is Apoptotic

(A, B) The *secA5-YFP* transgenic line detects annexin V activation. **(A)** Control embryos exhibit low levels of AnnexinV$^+$ cells (white dots, arrows). **(B)** In contrast, AnnexinV-YFP$^+$ apoptotic cells are abundant in cranial regions (arrows) following ethanol exposure. Higher magnification (insert) of Annexin-V-YFP$^+$ cells reveals the ring-shaped appearance characteristic of this early apoptotic marker on the membrane surface. **(C–E)** TUNEL$^+$ Staining. Control embryos **(C)** have few TUNEL$^+$ cells within cranial and other regions (arrows). In contrast, ethanol treatment **(D)** significantly increases TUNEL$^+$ cell abundance within cranial regions (arrows) and more caudal populations. **(E)** Embryo pretreatment with the CaMKII inhibitor myristoylated-AIP prevents the ethanol-induced apoptosis. **(F, G)** Quantitation of Ethanol-Induced Apoptosis. The number of Annexin-V-YFP$^+$ cells **(F)** and TUNEL$^+$ cells **(G)** were significantly increased within cranial regions following ethanol exposure as compared with controls. Values represent the mean ± SEM of 2–4 independent experiments, each having 6–10 (TUNEL) or 20–25 (Annexin-V) embryos per treatment. * $p<0.05$ vs. control using Kruskal-Wallis ANOVA on ranks. ** $p<0.001$ vs. control using two-tailed t-test.

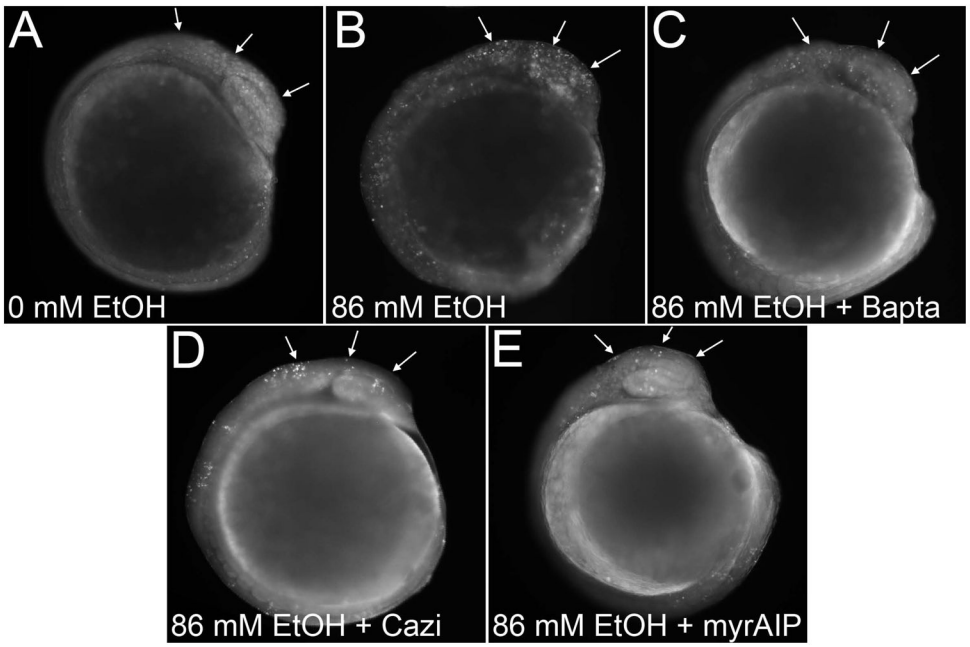

Figure 4. Ethanol-Induced Cell Death is CaMKII-Dependent

(A) Embryos exposed to 0mM ethanol have low cell death levels, assessed using acridine orange. **(B)** Cell death is significantly enhanced in embryos exposed to 86 mM ethanol (arrows). Ethanol-induced cell death in cranial regions is significantly reduced by pretreatment with the intracellular calcium chelator Bapta-AM **(C)**, the calmodulin inhibitor calmidizolium **(D)**, or the CaMKII inhibitor myristoylated-AIP **(E)**.

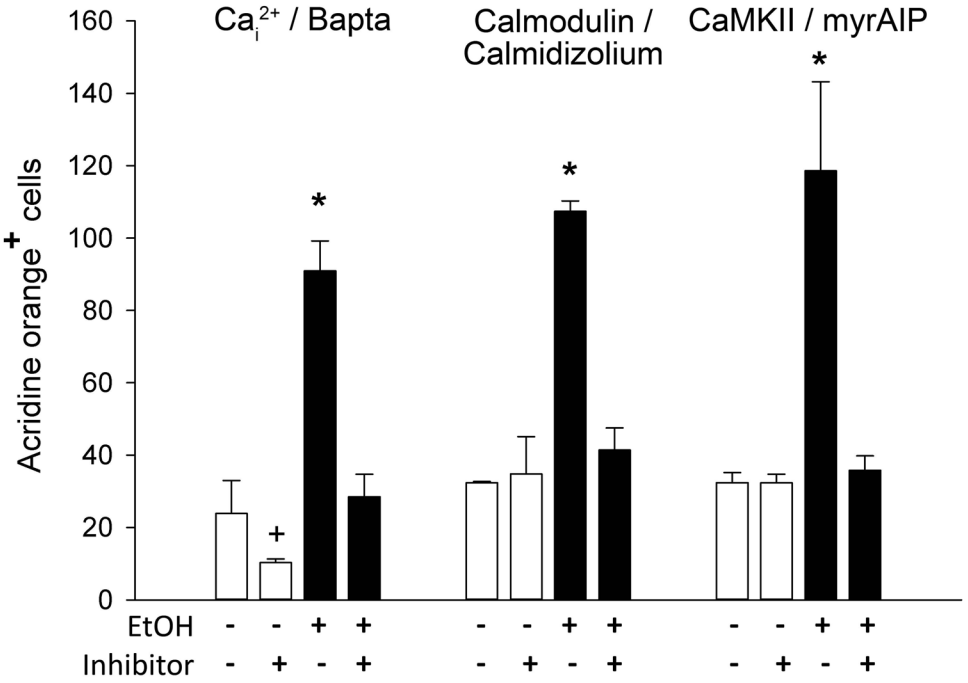

Figure 5. Quantitation of Calcium-Dependent Cell Death

Acridine orange$^+$ cells were enumerated in cranial region of embryos treated as indicated. Values represent mean ± SD of 2–3 independent experiments, each having 12–20 embryos per treatment. + p=0.041 and * p<0.001 vs. 0mM ethanol using one-way ANOVA followed by Holm-Sidak comparison.

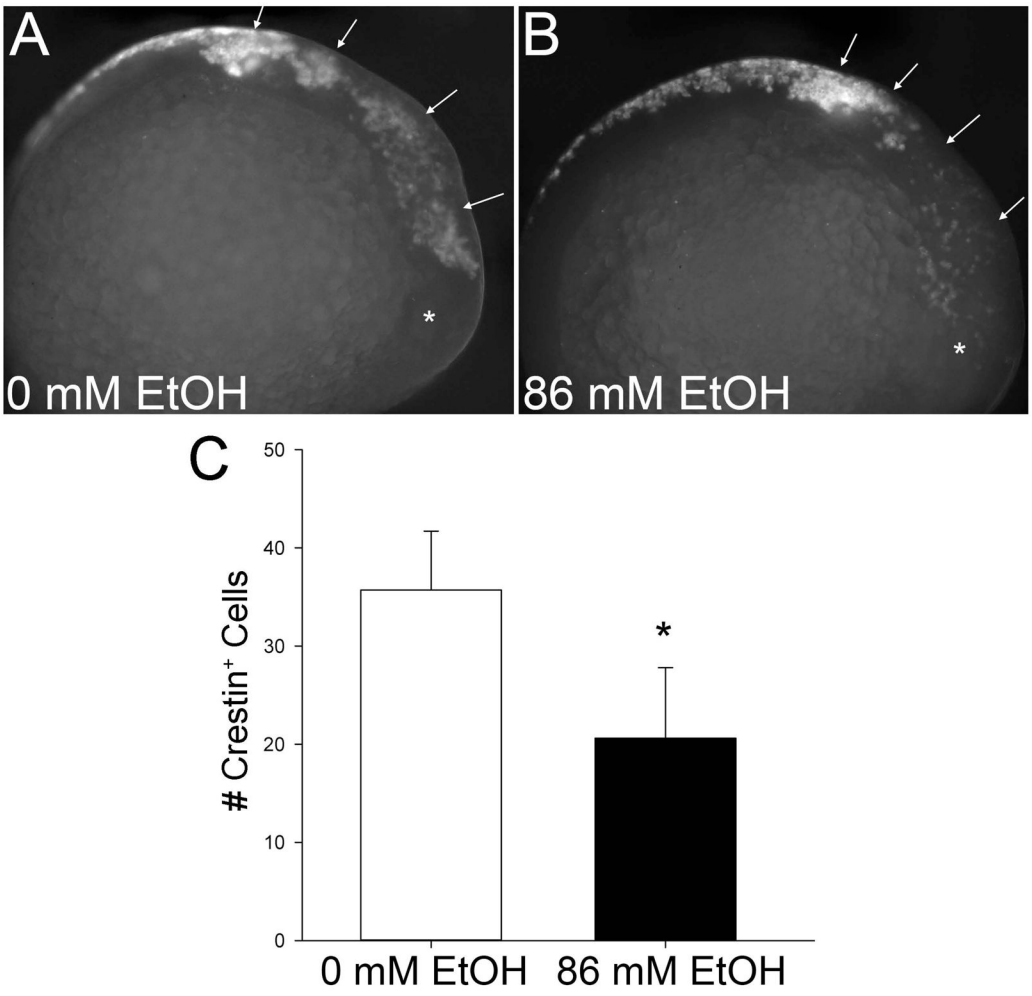

Figure 6. Ethanol Reduces Neural Crest Cellularity

Neural crest populations were visualized using *in situ* hybridization for *crestin* expression in embryos treated 3hr with 0mM **(A)** or 86mM ethanol$_{ext}$ **(B)**. Stage-matched embryos are shown. Arrows indicate cranial neural crest populations; * indicates the developing eye. **(C)** Quantitation of neural crest populations. The numbers of *crestin*$^{+}$ cells within the cranial region were counted. Values represent the mean ± SD of 3–5 embryos per treatment. * $p<0.001$ using two-tailed t-test.

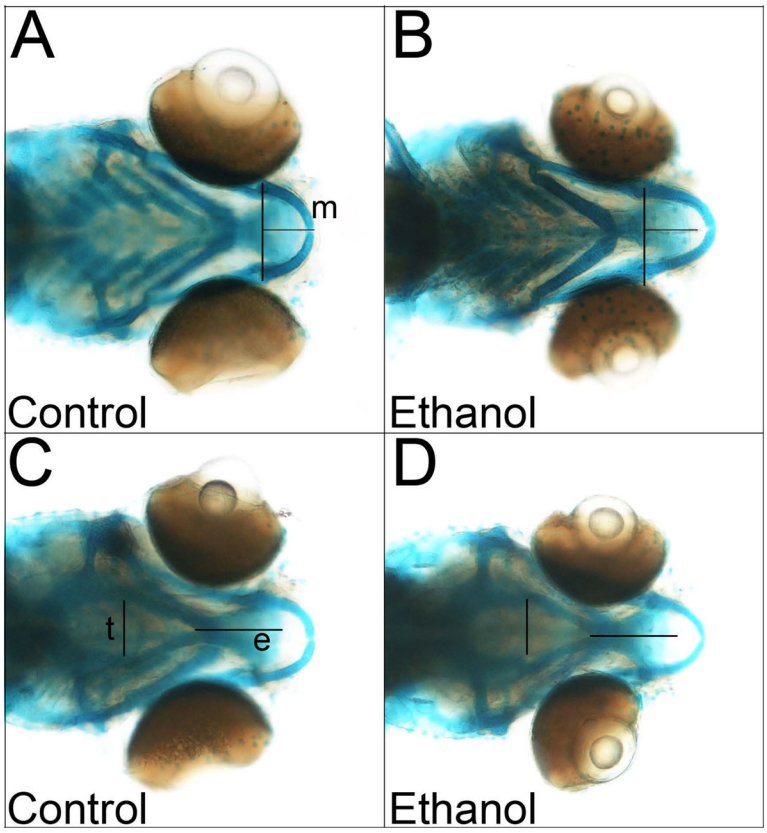

Figure 7. Ethanol Alters Craniofacial Structures

Skeletal elements of control or ethanol-treated zebrafish larvae at 6-days post-fertilization, viewed in ventral **(A)** or dorsal **(B)** aspect. Lines indicate cartilage dimensions significantly altered by ethanol; control dimensions are overlayed onto ethanol to highlight their differences. (e) ethmoid plate, (m) mandibular cartilage, (t) trabeculae crania.

Table 1

Effect of Washing on Ethanol Content

Treatment[†]	**$Ethanol_{int}$, mM**	**% of prior content**
0 mM ethanol	0.8 mM ± 0.5 mM	
171 mM ethanol (1% v/v)		
5 sec wash	55.8 mM ± 2.1 mM	
1 × 60 sec wash	26.6 mM ± 4.6 mM	47.7%
2 × 60 sec wash	11.4 mM ± 0.5 mM	42.9%

[†]Chorionated embryos were incubated 1hr in 171mM ethanol prior to washing and analysis. N = 25 embryos/group, assayed in triplicate, and 3 groups/treatment.